



ELSEVIER

Available online at www.sciencedirect.com

SCIENCE @ DIRECT®

Palaeogeography, Palaeoclimatology, Palaeoecology 219 (2005) 71–86

PALAEO

www.elsevier.com/locate/palaeo

Production and cycling of natural microbial exopolymers (EPS) within a marine stromatolite

Alan W. Decho^{a,*}, Pieter T. Visscher^b, R. Pamela Reid^c

^a*Department of Environmental Health Sciences, Arnold School of Public Health, University of South Carolina, Columbia, SC 29208, United States*

^b*Department of Marine Sciences, University of Connecticut, 1084 Shennecossett Rd., Groton, CT 06340, United States*

^c*Rosenstiel School of Marine and Atmospheric Science, Division of Marine Geology and Geophysics, University of Miami, 4600 Rickenbacker Causeway, Miami, FL 33149-1098, United States*

Received 3 June 2004; accepted 29 October 2004

Abstract

Extracellular polymeric secretions (EPS) that are produced by cyanobacteria represent potential structuring agents in the formation of marine stromatolites. The abundance, production, and degradation of EPS in the upper layers of a microbial mat forming shallow subtidal stromatolites at Highborne Cay, Bahamas, were determined using ¹⁴C tracer experiments and were integrated with measurements of other microbial community parameters. The upper regions of a Type 2 [Reid, R.P., Visscher, P.T., Decho, A.W., Stolz, J., Bebout, B., MacIntyre, I.G., Dupraz, C., Pinckney, J., Paerl, H., Prufert-Bebout, L., Steppe, T., Des Marais, D., 2000. The role of microbes in accretion, lamination and early lithification of modern marine stromatolites. *Nature (London)* 406, 989–992] stromatolite mat exhibited a distinct layering of alternating “green” cyanobacteria-rich layers (Layers 1 and 3) and “white” layers (Layers 2 and 4), and the natural abundance of EPS varied significantly depending on the mat layer. The highest EPS abundance occurred in Layer 2. The production of new EPS, as estimated by the incorporation of ¹⁴C-bicarbonate into EPS, occurred in all layers examined, with the highest production in Layer 1 and during periods of photosynthesis (i.e., daylight hours). A large pool (i.e., up to 49%) of the total ¹⁴C-bicarbonate uptake was released as low molecular-weight (MW) dissolved organic carbon (DOC). This DOC was rapidly mineralized to CO₂ by heterotrophic bacteria. EPS degradation, as determined by the conversion of ¹⁴C-EPS to ¹⁴CO₂, was slowest in Layer 2. Results of slurry experiments, examining O₂ uptake following additions of organic substrates, including EPS, supported this degradation trend and further demonstrated selective utilization by heterotrophs of specific monomers, such as acetate, ethanol, and uronic acids. Results indicated that natural EPS may be rapidly transformed post-secretion by heterotrophic degradation, specifically by sulfate-reducing bacteria, to a more-refractory remnant polymer that is relatively slow to accumulate. A mass balance analysis suggested that a layer-specific pattern in EPS and low-MW DOC turnover may contribute to major carbonate precipitation events within stromatolites. Our findings represent the first estimate of EPS

* Corresponding author. Fax: +1 803 777 6584.

E-mail addresses: awdecho@gwm.sc.edu (A.W. Decho), visscher@uconnvm.uconn.edu (P.T. Visscher), preid@rsmas.miami.edu (R.P. Reid).

turnover in stromatolites and support an emerging idea that stromatolite formation is limited by a delicate balance between evolving microbial activities and environmental factors.

© 2004 Elsevier B.V. All rights reserved.

Keywords: EPS; Bacteria; Cyanobacteria; Stromatolite; Production; Degradation; Biofilm

1. Introduction

Marine stromatolites represent a biogenic system that is of significant interest to geologists, microbiologists, and ocean chemists. Stromatolites are laminated sedimentary structures produced by microbial organisms (Awramik, 1992). Fossil stromatolites represent the earliest macroscopic evidence of life in the fossil record (Schopf, 1996). The microbial communities that produced these structures may have been instrumental in the generation of atmospheric oxygen (Des Marais, 1991; Knoll, 1992). The microorganisms forming stromatolites, thought to be mainly cyanobacteria and associated heterotrophic bacteria, were the dominant life forms for over 80% of the history of life on earth, forming extensive microbial reefs throughout the shallow waters of Precambrian oceans (Awramik, 1992). Stromatolites abruptly declined in the fossil record with the concurrent emergence of multicellular life approximately 600 my b.p. (Grotzinger, 1990; Knoll, 1992; Grotzinger and Knoll, 1999). Modern stromatolites, with living cyanobacterial surface mats, were discovered in a hypersaline environment in Shark Bay in Western Australia (Logan, 1961; Davis, 1970; Hoffman, 1976) and more recently in open marine conditions along the margins of Exuma Sound in the Bahamas (Dravis, 1983; Dill et al., 1986; Reid and Browne, 1991; Reid et al., 1995). These microbial mats provide a valuable system for examining the microbiogeochemical interactions involved in stromatolite formation and the precipitation of CaCO₃ (Stolz, 2000).

Recent studies of a wide range of the well-laminated, shallow, subtidal stromatolites at Highborne Cay, Bahamas (76° 49'W; 24° 43'N), have revealed that three major microbial mat types, representing a continuum of growth stages, can be defined (Reid et al., 2000). Type 1 mats are characterized by sparse populations of the cyanobacterium *Schizothrix* and

resemble pioneer communities (Stal, 1991, 1995). These dominate during periods of rapid sediment accretion. Type 2 mats represent a more mature surface community characterized by the development of a continuous surface film of extracellular polymeric secretions (EPS) and the development of a spatially-organized biofilm community. Type 3 mats are more fully-developed and in a more advanced developmental stage and include an abundant population of the boring coccoid cyanobacterium *Solentia* sp. This represents a climax community of the stromatolite system, and the microboring and calcification activities of the *Solentia* sp. result in laterally-cohesive carbonate crusts, which supports the longer-term preservation of the stromatolite (Reid et al., 2000).

High molecular-weight (MW) extracellular polymeric secretions (EPS) that are produced by cyanobacteria (Decho, 1990) may represent potentially important structuring agents in marine stromatolites (Decho, 2000). EPS serve to physically stabilize microbial cells against the high-energy environments (e.g., waves, tidal currents) that these structures commonly experience (De Winder et al., 1999; De Brouwer et al., 2002). Further, they may provide a chemically protective microenvironment for cells. They serve to bind and concentrate Ca²⁺ and Mg²⁺ ions from the surrounding seawater. The high abundance of EPS may effectively chelate large amounts of dissolved Ca²⁺ ions, perhaps preventing the precipitation of CaCO₃ (Kawaguchi and Decho, 2002a). Similarly, the degradation of EPS by heterotrophic bacteria may release Ca²⁺ and influence CaCO₃ precipitation.

The activities of different microbial functional groups within stromatolites in the Exuma Cays, Bahamas, appear to influence the precipitation of microcrystalline calcium carbonate (micrite) in distinct horizons (Pinckney et al., 1994; Visscher et al., 1998; MacIntyre et al., 1996, 2000). This precipitation results in the formation of lithified layers.

Confocal scanning laser microscopy (CSLM) and vacuum and environmental scanning electron microscopy (ESEM) studies indicate that lithified micritic horizons within Exuma stromatolites are in a proximate spatial association with dense layers of the filamentous cyanobacterium, *Schizothrix* sp. (Decho and Kawaguchi, 1999; Reid et al., 1999). However, recent studies using microautoradiography (Paerl et al., 2001) indicated that the aragonite needles (in the laminae) are closely associated with sulfate-reducing bacterial activities (Visscher et al., 1999, 2000). Some micritic horizons are also characterized by an abundance of the coccoid cyanobacterium, *Solentia* sp. (Visscher et al., 1998; MacIntyre et al., 2000). Micrite precipitation within these cyanobacteria-rich layers may be closely coupled with the activities of heterotrophic bacteria, either aerobic or anaerobic, and the production and degradation of EPS.

The purpose of this study was to examine the abundance, production, and degradation of microbial EPS within living marine stromatolites at Highborne Cay, Bahamas. The abundance of EPS material in different layers of a stromatolite mat was determined to establish levels of EPS with respect to resident photosynthetic organisms. The production of “newly-secreted EPS” was examined over a diel cycle using ^{14}C tracer experiments and slurry experiments to determine when highest EPS production occurred. The concomitant degradation of cyanobacterial EPS by heterotrophic bacteria was also examined. These data were used to establish a mass balance of EPS material within the stromatolite mat.

2. Methods

2.1. Sample descriptions

Samples of microbial mat were collected from the surface of a shallow subtidal stromatolite (Sample # 6/97 NS.8n) on the east beach of Highborne Cay, Bahamas (24 42.596°N; 76 49.372°W). The Highborne Cay study site was described in detail by Reid et al. (1999, 2000). The stromatolite mats were subsampled into 1 cm × 1 cm (diameter × depth) cores, which were used for all experiments. Under low magnification microscopy, four major layers were easily distin-

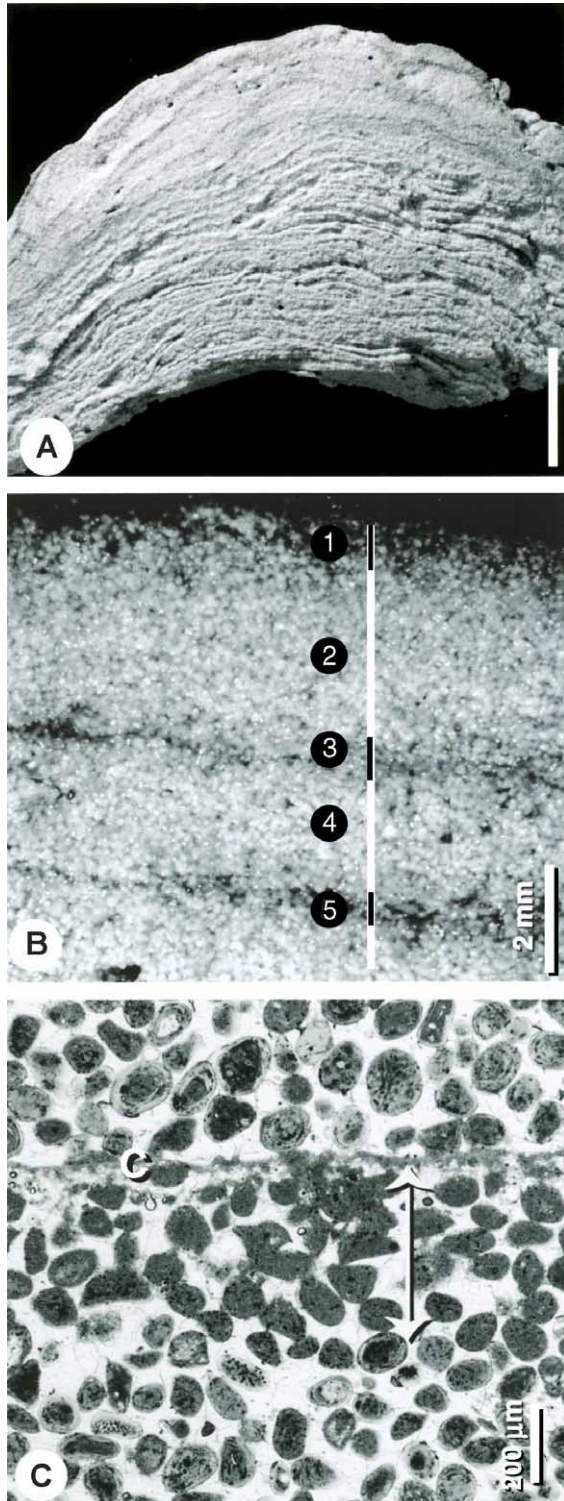
guished (Fig. 1b). See Reid et al. (2000) for a more detailed description of the mat layers. These were: (1) *Layer 1*, an unlithified caramel layer approximately 1 mm thick with an upper EPS-rich film (referred to as Layer 1A) underlain by a thin but dense layer of cyanobacteria (referred to as Layer 1B); (2) *Layer 2*, a white layer, 3–5 mm thick, which was unlithified and very cohesive and spongy in texture; (3) *Layer 3*, a dark, crusty, grey–green layer, which was relatively thin (1–2 mm) and was dominated by *Schizothrix* sp., but also contained abundant coccoid cyanobacteria *Solentia* sp., *Microcoleus* sp., and *Oscillatoria* sp.; and (4) *Layer 4*, a white layer which was relatively thick (3–5 mm) and was cohesive and spongy in texture. The microbial composition of this mat is described by Stolz et al., (in prep.).

2.1.1. Direct counts of bacteria

After the separation of the individual Layers 1–5 (see above), samples were fixed in buffered formaldehyde (2% final concentration, pH 7.5). The fixed samples of known volume were then subjected to dilute HCl (1 N) treatment, until the CaCO_3 was dissolved. The solution was then filtered onto destained Nuclepore membrane filters (0.45 μm) under mild vacuum. During filtration, acridine orange (163 μM) was added. Counts of fluorescent cells were made using an Olympus Vanox microscope. At least 1400 cells and two replicate samples per layer were counted.

2.1.2. Quantification of natural EPS material

The seawater (38 ppt salinity) and stromatolite mats used in experiments were collected from Highborne Cay, Bahamas. All glassware used in the below-described procedures was acid cleaned (10% HCl), then rinsed five times in deionized water and air-dried. Three replicate samples were used for the determinations of EPS abundance from each mat layer. Mat layer samples were placed into separate scintillation vials, then lightly homogenized into separated sand grains using a blunt plastic probe. EPS material was initially extracted by mixing from the mat material with ethylenediamine tetra-acetic acid (EDTA in seawater; 4 mM final concentration) and heating to 40 ± 1 °C for 15 min, with occasional stirring. This solubilization of EPS did not lyse the cyanobacterial cells. The suspended material, containing cells, detritus, and



EPS, was placed in a microcentrifuge tube and centrifuged ($8000\times g$, 6 min) to pellet cells and particulate detritus. The resulting supernatant, containing the EPS, was removed, was mixed with 70% (final concentration) cold ($4\text{ }^{\circ}\text{C}$) ethanol for 8 h. The pellet and remaining sediment were extracted using EDTA and heating as described above. This procedure was repeated three times. Preliminary experiments showed that no extractable EPS remained after three extractions. Precipitated material from the supernatant was collected by centrifugation, then redissolved in deionized H_2O . The ethanol precipitation was repeated twice, then the EPS was dialyzed (12,000 MWCO) against several changes of deionized H_2O using “Slid-A-Lyzer” microdialysis cassettes (Pierce Biochem.) for 24 h. EPS was lyophilized to dryness and stored at $-70\text{ }^{\circ}\text{C}$ until use. The sediments from the sample were washed with deionized H_2O to remove salts and loose detritus and were dried for the determination of sediment dry weights. All EPS samples were standardized according to sediment dry weight.

The quantification of EPS material was conducted by two different methods: the phenol–sulfuric acids method (Dubois et al., 1956; Liu et al., 1973; Underwood et al., 1995) and by total EPS dry weight. D-Glucose and alginic acid were used to obtain the standard curves for spectrophotometric determinations. C:N ratios of EPS material were also determined using Lehman Labs Model CE440 automated organic elemental analyzers (Dr. R. Petty, Univ. Calif., Santa Barbara). Results were reported as weight percent of the element.

2.1.3. Diel production of new EPS material

The production of “New EPS” material in the stromatolite mat was examined over a 24-h (diel)

Fig. 1. Stromatolites, Highborne Cay. (A) Sawed section showing lamination, which is defined by lithified horizons, approx. 1 mm thick, that stand out in relief on the cut surface. Sample 6/97.NS.8p. (B) Microbial mat from the surface of stromatolite 6/97.NS.8n used in the experiments in this work. Four major layers are indicated: Layer 1 is subdivided into an upper caramel colored section (1A) and a lower section that is green–yellow (1B). Layer 3 is grey–green and crusty. Layers 2 and 4 are grey–white and soft and cohesive. (C) Thin-section photomicrograph showing characteristic microstructure of the lithified layers: A micritic crust (c) overlies a zone of micritized grains that are cemented together at point contacts (arrow). Sample 6/97.NS.8f.

cycle by tracing the uptake of ^{14}C -bicarbonate and its subsequent incorporation into the EPS. For these experiments, twenty-one individual 1 cm diameter cores of intact stromatolite mat were placed in precleaned 22 ml borosilicate scintillation vials, with polypropylene caps. Clean sand (cleaned with sodium hypochlorite, $3\times$ rinsed in distilled water) was added to the vials to completely surround, but not cover, the stromatolite cores. The vials were filled with seawater (i.e., no head space). At 6:00 am (i.e., sunrise), 50 μl of $\text{NaH}^{14}\text{CO}_3$ (1.20 μCi ; 30–60 mCi/mmol) was added to each vial. The sealed vials were randomly arranged and placed in a circulating water bath (to maintain ambient seawater temperature conditions) under ambient sunlight conditions. It was assumed that the added $\text{NaH}^{14}\text{CO}_3$ tracer reached all layers of the stromatolite equally during the incubations. A factor of 1.06 was used to correct for isotope discrimination against heavier ^{14}C during bicarbonate uptake (Paerl, 1997). A set of triplicate dark vials (wrapped in foil) was used as controls. Sediment dark-controls, containing clean sand and a section of stromatolite mat, were used to control for the non-specific uptake of ^{14}C (i.e., sorption of radiolabeled bicarbonate) to the sediment. Dark-controls were wrapped in aluminum foil to prevent light exposure and were collected at 12 and 24 h. All samples were analyzed for ^{14}C on a Packard TR2400 liquid scintillation system, using 10 ml Ecolite Scintillation cocktail (ICN BioChem.). Sample counting times varied and were continued until 10,000 total counts were obtained for each sample. Counting efficiency quenching was corrected for using the external standards ratio method. For each time treatment, triplicate samples were removed from the water bath after incubation times (T) of 4, 8, 12, 16, 20, and 24 h and were injected with buffered Formalin (2% final concentration v/v). Several parameters were measured for each sample.

2.1.3.1. Samples of overlying water. Aliquots of the overlying sample water, collected from stromatolite incubation vials, were removed, and the pH was determined to ensure that it was above 8.2. The water samples were then centrifuged (10,000 \times g; 10 min) to pellet the particulates. Activities, expressed as disintegrations per minute (DPM), were determined for

both pellet and supernatant. The following parameters were measured on the water (supernatant) and particulates (centrifuged pellet):

- (1) Total ^{14}C in water= ^{14}C including bicarbonate, measured after the addition of 0.01 M NaOH.
- (2) ^{14}C -DOC in water= ^{14}C present in water after acidification (HCl for 24 h).
- (3) Centrifuged pellet=uptake by water-column bacteria and detritus.

2.1.3.2. Stromatolite Layers. In the laboratory, each mat sample was carefully separated into individual layers using microscopy (as previously described). The EPS were extracted from each stromatolite layer using the methods described above. The following parameters were measured for each stromatolite layer:

- (1) ^{14}C -EPS Activity=ethanol-precipitated fraction from stromatolites extracted as previously described above.
- (2) Low-MW ^{14}C -DOC Activity=collected as ethanol-soluble fraction derived from stromatolite EPS extract (after centrifugation).
- (3) Sediment dry weight:=represented the dry weight of sediment collected from each layer. This was used to standardize EPS concentrations.

The free sediment remaining in the sample vials (which was used to surround the stromatolite core during incubations) was also assayed for ^{14}C activity. Dark-control DPM were subtracted from the treatment DPM.

2.1.4. Heterotrophic degradation of EPS

2.1.4.1. Isolation of ^{14}C -EPS. Radiolabeled EPS, to be used in the degradation experiments, was extracted from laboratory cultures of a *Schizothrix* sp. previously isolated from stromatolite mats collected at Highborne Cay. Cultures were grown in 100 ml of CHU-10 medium (Rippka et al., 1979) in “Sigma seawater” (Sigma, St. Louis; collected outer Gulf stream; 32 ppt salinity; pH 8.2; 33–35 $^{\circ}\text{C}$) using a 12 h/12 h light/dark cycle. Cultures were grown under fluorescent lamps (approx. 300 lx) at 23–24 $^{\circ}\text{C}$. During mid log-phase of growth,

$\text{NaH}^{14}\text{CO}_3$ (50 μCi ; activity=30–60 mCi/mM; ICN Radiochemicals) was added to the cultures and incubated for 14 days. EPS were extracted and purified using the methods described above. The composition of this EPS is described elsewhere (Kawaguchi and Decho, 2000, 2002b). The activities of labeled EPS were described as DPM of ^{14}C per μg EPS.

2.1.4.2. ^{14}C -EPS degradation experiments. EPS degradation experiments were performed to examine the aerobic heterotrophic decomposition of EPS material within specific layers of the stromatolite. The degradation of ^{14}C -labeled EPS substrates was assayed by the generation of $^{14}\text{CO}_2$. Intact stromatolite samples were prepared as described above, then ^{14}C -labeled *Schizothrix* EPS (activity= 2.6×10^9 DPM per μg EPS), or [^{14}C] D-glucose (250–360 mCi per mM; ICN Radiochemicals) as a control, was carefully injected into either Layer 2 or Layer 3 of the stromatolite using a 26-gauge needle. For each sample, two injections of 5 μl EPS solution were made, yielding a total activity of approximately 2.60×10^6 dpm (1.18 μCi) per stromatolite. The cores were placed in precleaned scintillation vials and surrounded with loose sand. The vials were filled with 10 ml seawater, which provided a 9–10 ml headspace for air exchange. Scintillation vial lids were fitted with input and output ports using teflon septa and were sealed with silicon. A fresh supply of air was slowly bubbled into the seawater using an electric aquarium pumps fitted with Tygon tubing and silicon sealant to a multiport adjustable airvalve, to regulate gas exchange to the vessels. This provided a slow, uniform bubbling of air within all incubation vials.

$^{14}\text{CO}_2$ was collected sequentially from each sample by bubbling the outflow air through CO_2 traps. The $^{14}\text{CO}_2$ trap for each stromatolite sample consisted of two sequentially arranged vials, each containing 5 ml of 1 M KOH. The outflow from the incubation vials was bubbled into the bottom of the first trap. Air collected in the first trap was bubbled into the bottom of the second trap. The KOH trap vials were removed at different time intervals (2, 4, 6, 8, 10, 12, 18, 24, 30, 36, 40, and 48 h) and were quickly replaced with new vials containing KOH solution. This allowed the contin-

uous and efficient capture by the two sequential trapping vials of radiolabeled CO_2 gas produced during respiration. The vials then were individually assayed for $^{14}\text{CO}_2$ activity by mixing with Ecolite scintillation cocktail, chilled (4 $^\circ\text{C}$) in darkness for 24 h, then assayed by LSC as described above. The CO_2 trapping efficiency of the two sequential vial set-up was determined by injecting ^{14}C -bicarbonate directing into triplicate incubation vials containing sterile seawater. Because of the substantial quenching activity of the KOH solution, external standards were used for conversion to DPM. The DPM derived from the two sequential vials collected at a given time interval were then combined to yield the $^{14}\text{CO}_2$ activity for that time interval. Results were plotted cumulatively as the percentage of added DPM (carbon) that was recovered as $^{14}\text{CO}_2$ over time.

2.1.4.3. Degradation of organic carbon in slurries. Mat Layers 1–3 were separated and slurries were prepared by homogenizing the individual layers and mixing the homogenate with an equal volume of filter-sterilized seawater collected from the site. The slurries (10–25 ml) were incubated at ambient temperature (26–28 $^\circ\text{C}$) while stirring in a dark PVC vessel without a headspace, and O_2 uptake upon organic substrate additions was measured for up to 1 h. Oxygen was measured with a glass microelectrode with a guard cathode (Unisense, Aarhus, Denmark), and stirring was briefly stopped during O_2 readings. The O_2 consumption was calculated from the initial slope of oxygen uptake and corrected for endogenous respiration. All organic substrate additions were repeated twice. Substrates (glucose, xylose, mannose, acetate, and ethanol) were added to a final concentration ranging from 2 to 35 μM , except for *Schizothrix* EPS, of which $1.67 \mu\text{g ml}^{-1}$ was added.

2.1.5. Statistical analyses

EPS abundance data were analyzed using a one-way analysis of variance (ANOVA) (SAS, 1985) to examine the effects of mat layers on EPS abundance. Total EPS weights and hexose-equivalent weights for each mat layer were compared using a two-way ANOVA. Multiple comparisons of significant treatment effects among means were deter-

mined *a posteriori* using Bonferroni tests. A two-way factorial design ANOVA was used to examine the effects of mat layer and incubation time on EPS production (Piegorisch and Bailer, 1997). If a two-way ANOVA result indicated that as a significant factor, then the factor was compared using simple linear contrasts, followed by Bonferroni's multiple contrast for modifying alpha values (SAS, 1985). Appropriate transformations of data values were conducted to ensure the validity of the parametric assumptions. All statistical analyses were conducted using the GLM module of the SAS statistical software package (SAS, 1985).

3. Results

3.1. Bacterial counts

Epifluorescence microscopy of total cell counts (Fig. 2) revealed that the highest bacterial population was associated with Layer 1 and that Layers 1 and 3 (4×10^6 and 7×10^5 cells cm^{-3} sediment, respectively) contained higher biomass than Layers

2 and 4 did (2×10^4 and 8×10^3 cells cm^{-3} sediment, respectively).

3.2. Natural EPS abundance

The mean concentrations of EPS varied depend on the stromatolite layer. A high abundance of EPS occurred in Layers 1a, 2, and 4, while low abundance was found in Layers 1b and 3. The highest mean abundance occurred in Layer 2 (0.707 ± 0.232 mg EPS/g sed dry wt; average \pm S.D.; $n=3$) (Table 1; Fig. 3). The lowest polymeric abundance occurred in Layer 3 (0.137 ± 0.055 mg EPS/g sed; $n=3$). This pattern of EPS abundance within each stromatolite layer was consistent across all replicate samples. Analysis of variance showed that the total weight of extractable EPS was significantly ($P=0.0024$) greater in all layers than hexose-equivalent weights, determined using the phenol-sulfuric acid method. The C:N ratio of EPS from different layers also varied with the highest C:N ratios (6.3, 8.1, 7.1) being observed in the top caramel layers (1a) and white layers (2 and 4), respectively (Table 1). The C:N ratios of *Schizothrix* sp. EPS extracted from the laboratory cultures, which were grown under similar conditions to the ^{14}C -EPS used in the degradation experiments, were 9.2 ± 0.1 ($0 \pm \text{S.E.}_0$; $n=3$).

3.3. Diel production of "New" EPS material

Total bicarbonate uptake and production of labeled EPS were closely coupled to the light period. Maximum bicarbonate uptake occurred at the 6:00 pm sampling time period, with 53% of the added bicarbonate label having been incorporated in cells, DOC, or EPS (Fig. 4). The percent recovery of added ^{14}C -label ranged between 84% and 96% for all incubations. The uptake of ^{14}C by dark controls accounted for 0.003% of added ^{14}C -label.

The production of newly-secreted EPS, as evidenced by the accumulation of ^{14}C -label in the EPS, occurred within 4 h after the initial addition of ^{14}C -bicarbonate label. The net EPS production peaked at 2:00 pm and decreased thereafter (Fig. 5). The decrease coincided with an increase in ^{14}C detected as CO_2 (Fig. 6). Maximum EPS production represented 7.56% of the total ^{14}C -bicarbonate taken up by

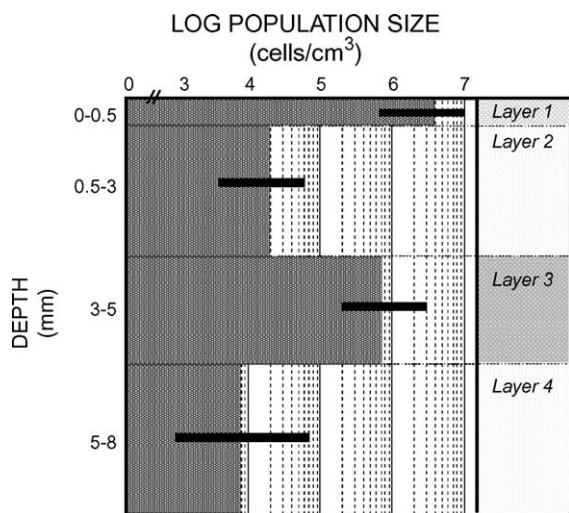


Fig. 2. Abundances of bacteria (AODC) associated with NS.8 stromatolite mat layers. The average of two replicate samples and error bar (\pm standard deviation) is provided for the top 4 layers. Cell densities (logarithmic scale) peak at the surface and are two to three orders of magnitude higher in lithified Layers 1 and 3 than in non-lithified Layers 3 and 4.

Table 1

Abundance and C:N ratios of natural extracellular polymeric material (EPS) collected from stromatolite mat layers

Stromatolite layer/color	EPS abundance (mg EPS/g dry sed)				
	Depth (cm)	Dry weight	Hexose-equivalent	Ratio Hx.Eq/EPStweight ^a	EPS C:N ratio
1 A (caramel)	0–0.1	0.620±0.030	0.453±0.06	0.73	6.3±0.02
1 B (green–yellow)	0.1–0.3	0.340±0.090	0.101±0.01	0.29	3.6±0.01
2 (white)	0.3–1.0	0.707±0.013	0.434±0.08	0.61	8.1±0.02
3 (dark–green)	1.0–1.5	0.137±0.031	0.032±0.02	0.23	2.4±0.01
4 (white)	1.5–2.0	0.551±0.020	0.346±0.10	0.63	7.1±0.01

EPS abundances and C:N ratios are expressed as mean±S.E. ($n=3$). EPS abundances are expressed as “Total EPS weight (mg)/g dry sediment”, and as “hexose-equivalent wt./g dry sediment” as estimated by the phenol–sulfuric acid method.

^a Ratio of hexose-equivalent EPS/EPS dry wt.

cells. The ¹⁴C in the extractable EPS decreased progressively between 6:00 pm and 6:00 am (i.e., during darkness) (Fig. 5).

3.4. Heterotrophic decomposition of EPS

The results of the degradation experiments to examine the decomposition of ¹⁴C-EPS added to Layers 2 and 3 in the stromatolite mat are shown in Fig. 7. The recovery efficiencies of added ¹⁴C-bicarbonate by dual KOH traps were 92% to 95%. During the first 6 h of incubation, only a low fraction (<7%) of the added ¹⁴C-EPS was degraded to ¹⁴CO₂.

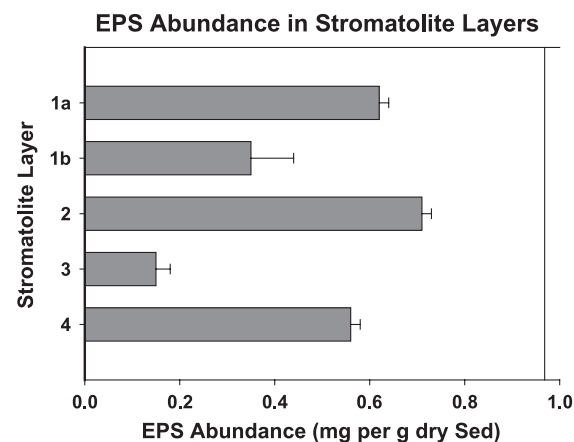


Fig. 3. Abundance of EPS material in stromatolite mat layers as determined by total dry weight EPS, and as glucose equivalent mass using the phenol–sulfuric acid method. Error bars represent standard error of mean ($n=3$).

The degradation proceeded rapidly after 6-h incubation, with a cumulative increase in ¹⁴CO₂ until 40 h. After 40 h, no major increase in cumulative ¹⁴CO₂ generation was observed. Approximately 50% of EPS was degraded within Layer 3 (as indicated by ¹⁴CO₂ production), and 37% within Layer 2 (Fig. 7). Controls, using ¹⁴C D-glucose, were more rapid and efficient (c.a., 70–80% respired) in conversion to ¹⁴CO₂ than EPS treatments were.

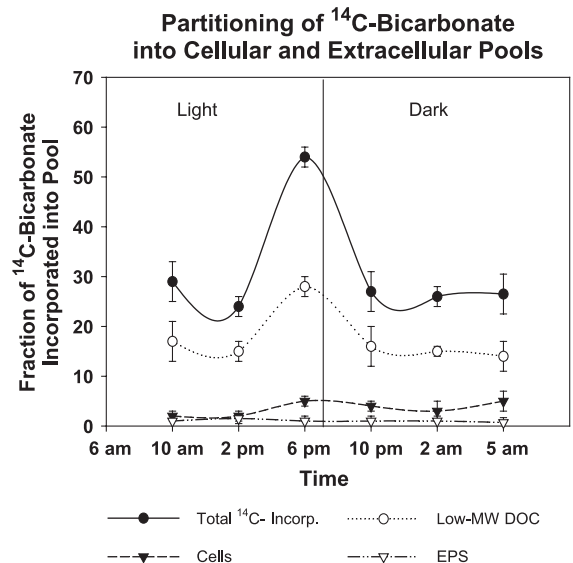


Fig. 4. Partitioning of ¹⁴C-bicarbonate into major cellular and extracellular pools during the 24-h diel production experiment. Note that a relatively large fraction of ¹⁴C incorporation is released as low-MW DOC.

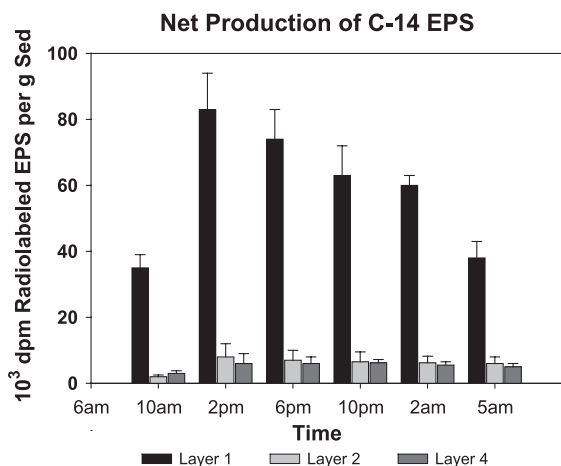


Fig. 5. Diel production by photosynthetic bacteria of newly-secreted ¹⁴C-EPS in three upper layers of a stromatolite mat. ¹⁴C-bicarbonate was added to stromatolite mats at 6 am (i.e., sunrise; 0-h incubation time), and its incorporation into extractable EPS was followed over a 24-h period; dpm=disintegrations per minute.

The addition of organic substrates resulted in a 5–10 fold increase of aerobic respiration in slurried mat samples (Table 2). Oxygen uptake rates were the highest in the slurries of Layer 1, and the lowest in the slurries of Layer 2. The stimulation of oxygen

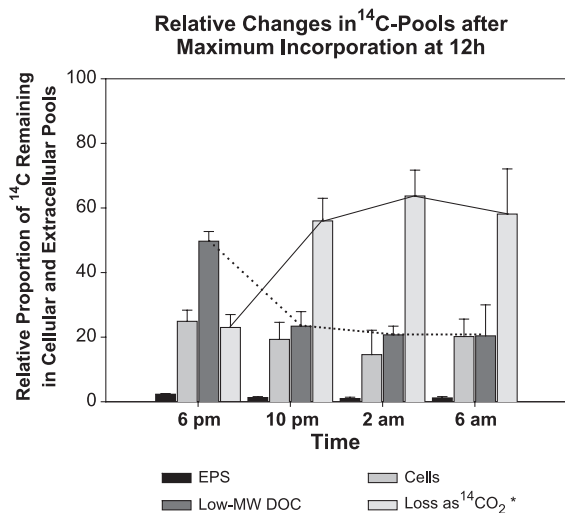


Fig. 6. Relative changes in cellular and extracellular ¹⁴C pools after maximum incorporation at 12-h incubation time. Note the rapid decrease in low-MW DOC after 6 pm, and a concurrent increase in CO₂, due to the conversion of DOC by heterotrophs.

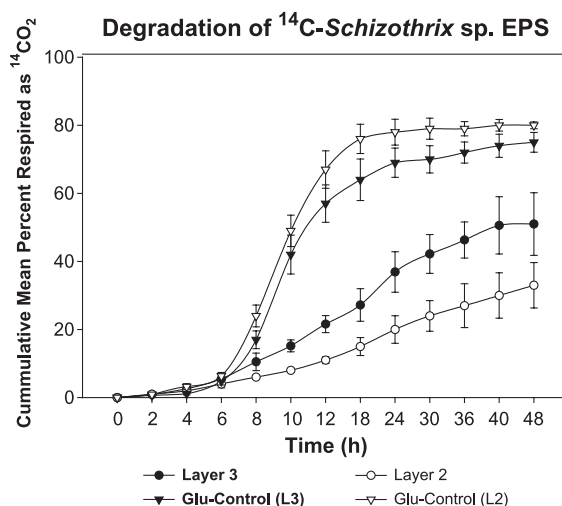


Fig. 7. Heterotrophic degradation over a 48-h period of ¹⁴C-EPS into ¹⁴CO₂. Tracer concentrations of ¹⁴C-EPS were injected into intact stromatolite mat layers, and the cumulative evolution of ¹⁴C respired as ¹⁴CO₂ was followed. Glu-control represents the ¹⁴C-glucose (control) injected into the mat.

uptake was higher upon the addition of acetate and ethanol (87–207 and 78–184 μmol ml⁻¹ slurry h⁻¹, respectively) than when EPS, glucose, mannose, or xylose was added (26–78, 35–101, 68–93, and 42–107 μM ml⁻¹ slurry h⁻¹, respectively). Substrate consumption started within 1 min upon addition, as was evident by decreasing oxygen concentration. An exception was EPS, which required a lag phase of 30–40 min before O₂ consumption increased over its endogenous rate.

Table 2

Aerobic respiration (O₂ uptake) after the addition of organic substrates in slurries prepared from individual mat layers of a stromatolite (NS.8), Highborne Cay, Bahamas

Carbon source	O ₂ uptake rate (d[O ₂]/dt) (μmol ml ⁻¹ h ⁻¹)		
	Layer 1	Layer 2	Layer 3
Acetate	207 (±11)	87 (±13)	172 (±13)
Ethanol	184 (±25)	78 (±11)	155 (±13)
Glucose	101 (±14)	35 (±4)	78 (±7)
Xylose	107 (±10)	42 (±10)	64 (±8)
Mannose	93 (±14)	n.d.	68 (±14)
EPS	78 (±8)	26 (±4)	51 (±4)
Endogenous rate	16 (±3)	8 (±1)	18 (±2)

Numbers are mean O₂ uptake rates (standard deviation is shown in parentheses). n.d.=not determined.

4. Discussion

The mat examined in our study at Highborne Cay is one example of stromatolites under current investigation. Reid and colleagues have examined a wide range of stromatolite mats and their associated microbial communities (Reid et al., 2000). They characterized three major types of surface communities, which occur along a continuum and exhibit varying degrees of precipitation. These range from rapidly-accreting, non-lithifying mats (Type I) to lithifying mats having a thin surface (and sometimes subsurface) crusty layer(s) (Type II) to strongly laminated (Type III) mats having thick laminae with fused grains. The current study examined sample 6/97 NS.8 (an early stage Type II mat) to determine how EPS and its microbial processes may be associated with lithification processes. This mat had a distinct surface crust present.

The rates at which microbial EPS are produced and degraded may represent an important varying factor influencing calcification within a stromatolite mat. In mats where there is high photosynthetic production, there may be a correspondingly high production of EPS. A high continued production of EPS would result in “spongy or gelatinous” stromatolite mats in which little or no lithification appears to be occurring. If EPS production exceeds EPS degradation (i.e., net accumulation of EPS), much of the Ca^{2+} ions would be bound (assuming that available ligands remain constant), making less Ca^{2+} available for precipitation. In contrast, a more rapid degradation of EPS and its associated heterotrophic microbial activities could release Ca^{2+} ions previously bound by EPS, making the ions potentially available for precipitation as CaCO_3 . Concentrated heterotrophic activities (i.e., EPS degradation and CO_2 production) and the concurrent release of Ca^{2+} ions within a mat layer may result in the localized precipitation of CaCO_3 and the formation of lithified layers.

Our results show that the abundance, degradation rates, and production rates of EPS varied significantly within the different layers of microbial mats forming stromatolites in Exuma Cays, Bahamas. Layers which had a relatively high natural abundance of EPS could have resulted from the relatively high production and/or slow degradation of EPS occurring in these layers. Layers that had a relatively lower abundance of EPS

generally exhibited more rapid EPS degradation rates. The observed differences in abundance, degradation, and production of EPS, and microbial composition, suggest that the Type II stromatolite mat is a very heterogeneous, vertically-layered system. This heterogeneity may contribute to the precipitation of distinct CaCO_3 micritic laminae associated with specific layers.

4.1. Bacterial cell counts

Direct cell counts of bacteria (Fig. 2) revealed that the highest population was associated with Layer 1. Also, Layers 1 and 3 contained higher biomass than Layers 2 and 4 did. The photosynthetic rates as measured by O_2 production during the light–dark and dark–light shifts with microelectrodes (Visscher et al., 1998) was the highest at 0.5–0.7 mm depth, which coincides with Layer 1. Thus, cyanobacterial production of oxygen and fixed carbon (including EPS and DOC) is associated with this depth interval, and therefore, the highest heterotrophic biomass can be sustained there. Aerobic respiration rates, also measured with microelectrodes, demonstrated that aerobic respiration peaked just below the depth of maximum O_2 production (Visscher et al., 1998). The relatively high biomass in Layer 3 is somewhat surprising, since O_2 penetrates only to the top of this layer and only during the peak of photosynthesis. Aerobic respiration could not be detected below Layer 2 (Visscher et al., 1998), but sulfate reduction and a population of sulfate reducers were associated with Layer 3 (Visscher et al., 1999). Therefore, the population of anaerobes, including sulfate-reducing bacteria, could account for the observed cell counts in this layer. Interestingly, the bacterial population of Layer 3 degraded ^{14}C -labeled EPS and glucose aerobically, and more rapidly so than did the microbes in Layer 2. Similarly, in the slurry experiments, the addition of monosaccharides and EPS stimulated O_2 uptake more so in the slurries of Layers 1 and 3, than the slurries of Layer 2. This indicates the presence of a viable aerobic heterotrophic population. In addition, sulfate reduction in the presence of O_2 has been reported in various microbial mats (Canfield and DesMarais, 1991; Fründ and Cohen, 1992; Visscher et al., 1992; Jørgensen, 1994), including Highborne Cay stromatolites (Visscher et al., 1999). The $^{14}\text{CO}_2$ production

can therefore be attributed to both aerobes and anaerobes.

4.2. Abundance of natural EPS material

Although the green layers (i.e., Layers 1, 3, and 5) contained high abundances of cells, EPS concentrations were significantly ($P=0.001$) lower (per gram dry sed) than the adjacent white layers did (i.e., Layers 2 and 4) (Fig. 2). Analyses of EPS concentrations using the phenol–sulfuric acid method (Dubois et al., 1956) showed that hexose sugars comprised a significantly ($P=0.0024$) smaller portion of EPS when compared with total EPS dry weights. The ratio of hexose-sugar abundance to total EPS dry weight varied depending on the layer (Table 1). This implies that a large portion (30–70% wt/wt) of the extractable EPS in the natural mat layers were composed of non-hexose sugar components. The variability in the C:N ratios of EPS extracted from the different layers also supported this idea. The highest C:N ratios (i.e., carbon-rich EPS) were observed in layers with higher EPS abundance (i.e., Layers 2 and 4) compared to layers with lower EPS abundance. Layers that showed the most rapid EPS degradation rates also showed lower C:N ratios (Table 1), when compared to adjacent layers. Together, these data suggest that over time, the carbohydrate (i.e., carbon) portion of stromatolite EPS is being partially or selectively degraded by heterotrophic microorganisms, leaving behind a more N-enriched residual polymer.

4.3. Diel “new production” of EPS material

The observed diel variation in the production of new EPS, as determined by the uptake of ^{14}C -bicarbonate by cells and its subsequent incorporation into EPS, showed that ^{14}C incorporation into EPS occurred very quickly (i.e., in less than 4 h). The highest production of EPS occurred during times when photosynthetic activities were also high (i.e., during daylight). A decrease in the total bicarbonate uptake was observed between 4 and 8 h incubation (i.e., 10:00 am to 2:00 pm), however (Fig. 4). This coincides with the period of highest solar irradiance and may represent a potential photoinhibition effect (Leverenz et al., 1990). Visscher et al. (1998)

observed that the highest rates of photosynthesis occurred before 2:00 pm. Decho et al. (in prep) observed the effects of varying light levels on the photosynthetic uptake of bicarbonate and its subsequent incorporation into EPS. They found that while EPS production occurred primarily during light conditions (i.e., associated with photosynthesis), the highest ambient levels of light reduced the production of EPS in the uppermost surface layer (0–0.2 mm depth). In the production experiments of the present study, this uppermost mat layer was not differentiated from Layer 1b. Therefore, any effects of photoinhibition on EPS production, if present, could not be discerned given our experimental design. The highest production of ^{14}C -labeled EPS occurred between 10:00 am and 2:00 pm (even though total bicarbonate uptake decreased during this same period), and the production of new EPS generally represented less than 3% to 4% of the total bicarbonate uptake by cells. Other studies of EPS production in phytoplankton (Mague et al., 1980; Wolter, 1982; Fogg, 1983; Myklesstad, 1998) showed that a relatively high percentage (i.e., 40–75%) of photoassimilate was used in mucilage production, and often in response to environmental stressors such as nutrient limitations. In contrast, studies of benthic diatoms showed that EPS production was not always directly linked to immediate photosynthetic assimilation of CO_2 (Cooksey and Cooksey, 1986; Smith and Underwood, 1998) but rather occurred primarily during migratory rhythms and tidal immersion of diatoms (Taylor and Paterson, 1998; Underwood and Kromkamp, 1999; Taylor et al., 1999; Smith and Underwood, 2000; Staats et al., 2000; De Brouwer and Stal, 2002). EPS production was influenced by irradiance levels (Wolfstein and Stal, 2002; Wolfstein et al., 2002) and could be further influenced by UV irradiation (Underwood et al., 1999).

Our data, derived from ^{14}C -bicarbonate production experiments, suggest that a large portion of the newly-produced EPS was rapidly (i.e., within 12 h after secretion) degraded by heterotrophs. We observed that the cumulative mean production of ^{14}C -EPS decreased after 8 h (i.e., dark portion) of the diel cycle (Fig. 5). This pattern was consistent across all replicates ($n=3$) for each time period and reduced the net production of EPS to less than 2% of the initial bicarbonate uptake by cells. We propose that approx-

imately 40% to 60% of newly-secreted EPS carbon is partially degraded and converted to CO₂ by heterotrophs. Our degradation studies, using ¹⁴C-labeled EPS, support this (see below) and suggested that 30–50% of added EPS carbon was degraded over a 48-h period, leaving behind a more-refractory portion of the EPS carbon.

Low MW DOC was a major carbon pool produced during the diel experiments (Fig. 4). The sampling time during which maximum ¹⁴C-bicarbonate was incorporated into organic cellular and extracellular pools occurred after 6:00 pm (Table 3). During this period, low-MW DOC represented 49.7±3.1% (mean±S.E.; n=3) of the total incorporated ¹⁴C-bicarbonate. The subsequent loss of ¹⁴C-label from the DOC pool during the next 4 h coincided with an increase in the fraction recovered as ¹⁴CO₂ (Fig. 6). These data strongly suggested that rapid degradation of ¹⁴C-DOC into ¹⁴CO₂ by heterotrophic bacteria occurred during two different time periods, between 10:00 am and 2:00 pm and between 6:00 pm and 10:00 pm, just after the conclusion of daylight. This infers a very close temporal and spatial coupling of photosynthetic production and heterotrophic utilization in the upper layers of the stromatolite mat. Since a net decrease in ¹⁴C-EPS was observed during 12-h to 24-h incubation, we assume that no major conversion by heterotrophic bacteria of ¹⁴C-DOC into ¹⁴C-EPS occurred. Most of the ¹⁴C-DOC was mineralized into ¹⁴CO₂. The rapid degradation of dissolved organic carbon, derived from planktonic sources such as diatom blooms and phytoplankton, has also been observed by a number of investigators

(Cho and Azam, 1988; Kirchman et al., 1991; Amon and Benner, 1994; Norman et al., 1995).

4.4. Degradation of EPS

The degradation of ¹⁴C-labeled EPS, derived from the cyanobacterium *Schizothrix* sp., varied depending on the stromatolite layer. The cumulative evolution of ¹⁴CO₂ resulting from the heterotrophic decomposition of ¹⁴C-EPS was best described by a third-order curve (Hu and Bruggen, 1997) over the 48-h time period. Initial degradation of ¹⁴C-EPS, after addition of label, was preceded by a 6-h lag period, in which there was no significant capture of ¹⁴CO₂. This lag could have resulted from: (1) the lack of degradation (uptake and hydrolysis of substrate) for the initial 6–8 h. This is not likely, however, since a similar 6–8 h lag was also observed in D-glucose controls (Fig. 7), and glucose represents an easily hydrolyzable substrate for many bacteria. (2) A more likely scenario is that much of the initial lag occurred because of ¹⁴CO₂ diffusion from the mat. (3) It is possible that isotopic dilution occurred over the 48-h time series (Sawyer and King, 1993; King, 1997). For this reason, it may be concluded that our experimental results provided a relatively conservative (i.e., slow) estimate of EPS degradation. Once ¹⁴CO₂ evolution was detectable, a rapid cumulative increase occurred and continued until approximately 40 h, after which time there was no net gain in ¹⁴CO₂. A mass balance of EPS turnover (to CO₂), as estimated directly from the ¹⁴C-EPS degradation experiments, was ca. 30–50% loss of C (as ¹⁴CO₂) over 48 h. Estimates determined indirectly from the ¹⁴C-EPS production experiments over 24 h were ca. 35–60%. The relatively close agreement of these two estimates suggests that a large portion of newly-produced EPS was degraded and ultimately respired by heterotrophs and further supports the idea that EPS was turned over rapidly in certain layers (e.g., Layers 1 and 3) of the stromatolite mat. Studies by Anderson et al. (1987) of hot spring Cyanobacterial mats showed that the dark fermentation of polymeric organic matter leads to the production of organic acids which supply heterotrophs. The partial and rapid degradation of newly-produced EPS may have reduced net accumulations to less than ca. 1% per day, even in the most active layers of the mat. In studies of other non-mat systems, the degradation of

Table 3

Summary table showing characteristics of processes within the upper mat layers of stromatolite “NS.8.n 6/97” and EPS-related processes that (may) favor potential precipitation of CaCO₃

Mat layer	Color	EPS prod.	EPS degrad.	EPS C:N	Net EPS abund.	Potential for major precip.
LAYER 1A	‘White’	HIGH	n.d.	HIGH	HIGH	YES
LAYER 1B	‘Yellow–green’			Low	Low	
LAYER 2	‘White’	Low	Slow	HIGH	HIGH	NO
LAYER 3	‘Green’	Low	FAST	Low	Low	YES
LAYER 4	‘White’	n.d.	n.d.	HIGH	HIGH	NO

n.d.=not determined.

EPS and other polymers in various forms have indicated generally slow turnover times (e.g., days to months) (Henrichs and Doyle, 1986; Weaver and Hicks, 1995; Hu and Bruggen, 1997).

In slurries of mat layers, the labile DOC was degraded at the highest rates. This is in agreement with the ^{14}C radiolabel experiments that revealed that the DOC pool was a major constituent of new production and that this carbon pool was turned-over rapidly. Interestingly, monosaccharides and EPS were oxidized equally fast by slurries as determined by O_2 uptake. From EPS: O_2 stoichiometry (data not shown), the O_2 consumption seems to level off before all EPS is completely degraded to CO_2 , similar to the $^{14}\text{CO}_2$ recovery experiment (Fig. 7). Both radiolabeling and slurry experiments showed a lag phase prior to a rapid consumption. This indicates that in contrast to labile DOC, induction or de-repression of hydrolytic enzyme systems is required. The slurry experiments had a much shorter lag than did the radiolabel study. In contrast to experiments with ^{14}C -labeled glucose in intact samples, the slurry experiments which have well-mixed conditions and initially contain O_2 to its saturation provide a maximum potential respiration rate. However, if organic substrates are only partially degraded, this is detected by O_2 uptake and not necessarily by $^{14}\text{CO}_2$ production. This suggests that a partial degradation of EPS may occur that does not yield CO_2 , perhaps the presence of relatively labile sidechains that degrade more rapidly. Alternatively, higher rates obtained in the slurry experiments could be due to the better mixing of the substrate EPS and/or the higher O_2 concentration present.

When calculating the specific O_2 uptake rates from the epifluorescence counts and slurry experiments, the rate for acetate is 1, 44, and 4 $\text{nM cell}^{-1} \text{h}^{-1}$, respectively, for Layers 1, 2, and 3. For glucose, the cell specific rates are 0.5, 18, and 1.3 $\text{nM cell}^{-1} \text{h}^{-1}$, and for EPS, 0.4, 13, and 1.3 $\text{nM cell}^{-1} \text{h}^{-1}$ in Layers 1, 2, and 3, respectively. The highest specific rates are clearly associated with Layer 2, which population seems to prefer labile organic compounds (acetate) to monosaccharides and EPS. The much higher rate per cell in Layer 2 indicates that the bacteria in that layer could be starved with respect to organic substrates. The relatively higher rates in Layer 3, in comparison to Layer 1, could be attributed to carbon consumption by other respiratory processes such as the sulfate

reduction that obviously is unaccounted for in O_2 consumption. The sulfide produced during sulfate reduction requires O_2 for its oxidation, but this oxidation is incomplete, yielding polythionates and elemental sulfur (Visscher et al., 2002; Van den Ende and Van Gemerden, 1993). Visscher et al. (1998, 1999) showed in an earlier study that in Layer 3, sulfate reduction accounted for a significant sink for organic carbon.

4.5. Mass balance of EPS turnover

The extracellular secretion of EPS and the release of a wide array of low-MW metabolic products by cyanobacteria provide a supply of readily-utilizable organic molecules to stimulate utilization by heterotrophic bacteria. We found that the bacterial degradation of EPS to CO_2 was more rapid in dark-green cyanobacteria-rich layers, when compared to adjacent white layers. This may have occurred because the abundance of organic molecules stimulated bacterial heterotrophy in this layer.

The abundances of EPS were significantly ($P < 0.001$) higher in white layers because both EPS production was relatively high and heterotrophic degradation was slower than in adjacent green layers. The rapid conversion of low-MW DOC by heterotrophic bacteria to CO_2 may be particularly important in funneling C production. Bateson and Ward (1988) observed rapid transfer of secreted low-MW DOC, specifically glycolate, from photosynthetically-active *Synechococcus* cells to filamentous Chloroflexus-like organisms in hot-spring cyanobacterial mats.

A simple mass balance of total ^{14}C cycling within Layers 2 and 3 of the stromatolite mat was constructed in order to estimate if there was a net-accumulation or net-decrease in EPS material within the different layers of the stromatolite mat. The mass balance was calculated where:

$$\text{Net EPS Accumulation (per24h)} = \text{EPS Production} \\ \times (24\text{h}) - \text{EPS Degradation (24h)}$$

The proportion of ^{14}C -bicarbonate that was taken up by autotrophic cells and incorporated into EPS during the incubation periods was determined. The degradation of newly-secreted EPS was estimated as the cumulative mean decrease in ^{14}C -EPS after its peak

production and was subtracted from this value. Net production, therefore, was a function of EPS production and degradation over a 24-h period. Net EPS accumulation values were determined for stromatolite Layers 2 and 3. Our results (Table 2) suggest that microbial heterotrophic activities (i.e., degradation) may influence the turnover of C to different extents, depending on the mat layer, and that the turnover process was dependent on microbial production in the upper layers (i.e., photosynthetic C production). The relative roles that aerobic and anaerobic heterotrophy play in carbon cycling are currently under investigation. The EPS pools of stromatolites, which are secreted largely by cyanobacteria (Kawaguchi et al., 2003), are partially degraded soon after secretion. The EPS-remnant may be compositionally different and less labile to microbial degradation and may constitute an important structuring agent in longer-term persistence of stromatolites.

Our data and others (Kawaguchi and Decho, 2002a,b) showed that natural biofilm EPS represent a “more-refractory remnant” of the original polymer molecule(s) that is initially secreted by photosynthetic microorganisms. Our findings also indicate that layer-specific differences in EPS turnover were present within stromatolites. In green layers (e.g., Layers 1 and 3), there was a net loss of EPS (i.e., EPS Degradation > EPS Production). Although the top layer (Layer 1) of the stromatolite mat showed the highest production of EPS, a more rapid degradation of EPS (and DOC) by heterotrophic bacteria also occurred. This may fuel a diel pattern of production/respiration that creates favorable conditions for the precipitation of CaCO₃. In the white layers (e.g., Layer 2) of stromatolites, there was a high abundance and net gain in EPS (i.e., EPS Production > EPS degradation). Although Layer 2 had a lower production of EPS, there was a slower degradation of EPS. This resulted in a slight net gain of EPS (i.e., EPS Production > EPS Degradation) over time. The higher net gain of EPS presents conditions (Ca⁺⁺ binding) that may reduce the capacity for major precipitation of micritic laminae.

Reid et al. (2000) presented a model of stromatolite formation. The model was derived from existing data and showed how microbial communities may develop through a series of successional stages (Types I and II), which may culminate in the formation of

regularly-spaced thick laminae (Type III). These laminae contribute to the longer-term stability of modern stromatolites and characterize fossil stromatolites. The model also emphasizes how intermittent environmental perturbations (e.g., sedimentation rate and burial events) and perhaps endogenous interactions may influence the continued succession development, or cessation, of stromatolite growth (Stal, 2000). A central role of microbial EPS in this process was proposed in the model, since EPS may contribute to sediment trapping, Ca²⁺ ion binding, and inhibition of calcification. The present study represents the first estimate of EPS turnover in a natural system and within stromatolites.

Acknowledgements

We acknowledge Drs. Hans Paerl, Timothy Stegge (Marine Sciences Institute, UNC-Chapel Hill, Morehead City, NC), and James Pinckney (Marine Sciences Program, USC, Columbia, SC) for their constructive discussions and input during this work. Thanks are extended to crew of the R.V. Calanus (University of Miami) for providing an efficient working environment during our cruise, and to the staff of the Highborne Cay Marina (Exumas, Bahamas). This work was supported by NSF grants (OCE 95-30215, 96-19314, and 96-17738; EAR-BE 0221796) and represents RIBS (Research Initiative on Bahamian Stromatolites) Contribution #25.

References

- Amon, R.M.W., Benner, R., 1994. Rapid cycling of high-molecular weight dissolved organic matter in the ocean. *Nature (Lond.)* 369, 549–552.
- Anderson, K.A., Tayne, T.A., Ward, D.M., 1987. Formation and fate of fermentation products in hot spring Cyanobacterial mats. *Appl. Environ. Microbiol.* 53, 2343–2352.
- Awramik, S.M., 1992. The history and significance of stromatolites. In: Schidlowski, M., et al. (Eds.), *Early Organic Evolution: Implications for Mineral and Energy Resources*. Springer-Verlag, Berlin, pp. 435–449.
- Bateson, M.M., Ward, D.M., 1988. Photoexcretion and fate of glycolate in a hot spring Cyanobacterial mat. *Appl. Environ. Microbiol.* 54, 1738–1743.
- Canfield, D.E., DesMarais, D.J., 1991. Aerobic sulfate reduction in microbial mats. *Science* 251, 1471–1473.

- Cho, B.C., Azam, F., 1988. Major role of bacteria in biogeochemical fluxes in the ocean's interior. *Nature* 332, 441–443.
- Cooksey, K.E., Cooksey, B., 1986. Adhesion of fouling diatoms to surfaces: some biochemistry. In: Evans, L.V., Hoagland, K.D. (Eds.), *Algal Biofouling: Studies in Environmental Science*, vol. 28. Elsevier.
- Davis, G.R., 1970. Algal laminate sediments, Gladstone embayment, Shark Bay, Western Australia. *Am. Assoc. Pet. Geol., Mem.* 13, 85–168.
- De Brouwer, J.F.C., Stal, L.J., 2002. Daily fluctuations of exopolymers in cultures of the benthic diatoms *Cylindrotheca closterium* and *Nitzschia* sp. (Bacillariophyceae). *J. Phycol.* 38, 464–472.
- De Brouwer, J.F.C., Ruddy, G.K., Jones, T.E.R., Stal, L.J., 2002. Sorption of EPS to sediment particles and the effect on the rheology of sediment slurries. *Biogeochemistry* 61, 57–71.
- Decho, A.W., 1990. Microbial exopolymer secretions in ocean environments: their role(s) in food webs and marine processes. *Oceanogr. Mar. Biol. Annu. Rev.* 28, 73–153.
- Decho, A.W., 2000. Microbial biofilms in intertidal systems: an overview. *Cont. Shelf Res.* 20, 1257–1273.
- Decho, A.W., Kawaguchi, T., 1999. Confocal imaging of natural in situ microbial communities and their extracellular polymeric secretions (EPS) using Nanoplast resin. *BioTechniques* 27, 1246–1251.
- Des Marais, D.J., 1991. Microbial mats, stromatolites and the rise of oxygen in the Precambrian atmosphere. *Palaeogeogr. Palaeoclimatol. Palaeoecol.* 97, 93–96.
- De Winder, B., Staats, N., Stal, L.J., Paterson, D.M., 1999. Carbohydrate secretion by phototrophic communities in tidal sediments. *J. Sea Res.* 42, 131–146.
- Dill, R.F., Shinn, E.A., Jones, A.T., Kelly, K., Steinin, R.P., 1986. Giant subtidal stromatolites forming in normal saline waters. *Nature* 324, 55–58.
- Dravis, J.J., 1983. Hardened subtidal stromatolites, Bahamas. *Science* 219, 385–386.
- Dubois, M., Gilles, K.A., Hamilton, J.K., Rebers, P.A., Smith, F., 1956. Colorimetric methods for determination of sugars and related substances. *Anal. Chem.* 28, 350–356.
- Fogg, G.E., 1983. The ecological significance of extracellular production of phytoplankton photosynthesis. *Bot. Mar.* 26, 3–14.
- Fründ, C., Cohen, Y., 1992. Diurnal cycles of sulfate reduction under oxic conditions in microbial mats. *Appl. Environ. Microbiol.* 58, 77.
- Grotzinger, J.P., 1990. Geochemical model for Proterozoic stromatolite decline. *Am. Sci.* 290, 80–103.
- Grotzinger, J.P., Knoll, A.H., 1999. Stromatolites in Precambrian carbonates: evolutionary mileposts or environmental dipsticks? *Annu. Rev. Earth Planet. Sci.* 27, 313–358.
- Henrichs, S.M., Doyle, A.P., 1986. Decomposition of ¹⁴C-labeled organic substances in marine sediments. *Limnol. Oceanogr.* 31, 765–778.
- Hoffman, P., 1976. Stromatolite morphogenesis in Shark Bay, Western Australia. In: Walter, M. (Ed.), *Stromatolites*. Elsevier Sci. Publ., Amsterdam, pp. 261–273.
- Hu, S., Bruggen, A.H.C., 1997. Microbial dynamics associated with multiphasic decomposition of ¹⁴C-labeled cellulose in soil. *Microb. Ecol.* 33, 134–143.
- Jørgensen, B.B., 1994. Sulfate reduction and thiosulfate transformation in a Cyanobacterial mat during a diel oxygen cycle. *FEMS Microbiol. Ecol.* 13, 303–312.
- Kawaguchi, T., Decho, A.W., 2000. Biochemical characterization of Cyanobacterial extracellular polymers from modern marine stromatolites. *Prep. Biochem. Biotechnol.* 30, 321–330.
- Kawaguchi, T., Decho, A.W., 2002a. Isolation and biochemical characterization of extracellular polymeric secretions (EPS) from modern marine stromatolites and its inhibitory effect on CaCO₃ precipitation. *Prep. Biochem. Biotechnol.* 32, 51–63.
- Kawaguchi, T., Decho, A.W., 2002b. A laboratory investigation of Cyanobacterial extracellular polymeric secretions (EPS) in influencing CaCO₃ polymorphism. *J. Crystal Growth* 240, 230–235.
- Kawaguchi, T., Al Sayegh, H., Decho, A.W., 2003. Development of an indirect competitive enzyme-linked immunosorbent assay to detect extracellular polymeric substances (EPS) secreted by the marine stromatolite-forming cyanobacterium, *Schizothrix* sp. *J. Immunoass. Immunochem.* 24, 29–39.
- King, G.M., 1997. Applications of ¹⁴C and ³H radiotracers for analysis of benthic organic matter transformations. In: Hurst, C.J., Hudson, G.R., McInerney, M.J., Stetzenbach, L.D., Walter, M.V. (Eds.), *Manual of Environmental Microbiology*. Amer Soc Microbiol Press, Washington, pp. 317–323.
- Kirchman, D.L., Suzuki, Y., Garside, C., Ducklow, H.W., 1991. High turnover rates of dissolved organic carbon during a spring phytoplankton bloom. *Nature (Lond.)* 352, 612–614.
- Knoll, A.H., 1992. The early evolution of eukaryotes: a geological perspective. *Science* 256, 622–627.
- Leverenz, J.W., Falk, S., Pilstrom, C.-M., Samuelsson, G., 1990. The effects of photoinhibition on the photosynthetic light-response curve of green plant cells (*Chlamydomonas reinhardtii*). *Planta* 182, 161–168.
- Liu, D., Wong, P.T.S., Dutka, P.J., 1973. Determination of carbohydrate in lake sediment by a modified phenol-sulfuric acid method. *Water Res.* 7, 741–746.
- Logan, B.W., 1961. Cryptozoan and associated stromatolites from the Recent, Shark Bay, Western Australia. *J. Geol.* 69, 517–533.
- MacIntyre, I.G., Reid, R.P., Stenek, R.S., 1996. Growth history of stromatolites in a Holocene fringing reef, Stocking Island, Bahamas. *J. Sediment. Res.* 66, 231–242.
- MacIntyre, I.G., Prufert-Bebout, L., Reid, R.P., 2000. The role of endolithic Cyanobacteria in the formation of lithified laminae in Bahamian stromatolites. *Sedimentology* 47, 915–921.
- Mague, T.H., Friberg, E., Hughes, D.J., Morris, I., 1980. Extracellular release of carbon by marine phytoplankton: a physiological approach. *Limnol. Oceanogr.* 28, 262–279.
- Mykkestad, S., 1998. Production, chemical structure, metabolism and biological function of the (1-3)-linked, ?-D-glucans in diatoms. *Biol. Oceanogr.* 6, 313–326.
- Norman, B., Zweifel, U.L., Hopkinson, C.S., Fry, B., 1995. Production and utilization of dissolved organic carbon during an experimental diatom bloom. *Limnol. Oceanogr.* 40, 898–907.

- Paerl, H.W., 1997. Primary productivity and producers. In: Hurst, C.J., Hudson, G.R., McInerney, M.J., Stetzenbach, L.D., Walter, M.V. (Eds.), *Manual of Environmental Microbiology*. Amer. Soc. Microbiol. Press, Washington, pp. 252–262.
- Paerl, H.W., Stepe, T.F., Reid, R.P., 2001. Microbially mediated lithification in marine stromatolites: who's responsible? *Environ. Microbiol.* 3, 123–130.
- Piegorsch, W.W., Bailer, A.J., 1997. *Statistics for Environmental Biology and Toxicology*. Chapman and Hall, NY, 579 pp.
- Pinckney, J., Paerl, H.W., Reid, R.P., Bebout, B., 1994. Ecophysiology of stromatolitic mats, Stocking Island, Exuma Cays, Bahamas. *Microb. Ecol.* 29, 19–37.
- Reid, R.P., Browne, K.M., 1991. Intertidal stromatolites in a fringing Holocene reef complex, Bahamas. *Geology* 19, 15–18.
- Reid, R.P., MacIntyre, I.G., Browne, K.M., Steneck, R.S., Miller, T., 1995. Modern marine stromatolites in the Exuma Cays, Bahamas: uncommonly common. *Facies* 33, 1–18.
- Reid, R.P., MacIntyre, I.G., Steneck, R.S., 1999. A microbialite/algal ridge fringing reef complex, Highborne Cay, Bahamas. *Atoll Res. Bull.* 465, 1–18.
- Reid, R.P., Visscher, P.T., Decho, A.W., Stolz, J., Bebout, B., MacIntyre, I.G., Dupraz, C., Pinckney, J., Paerl, H., Prufert-Bebout, L., Stepe, T., Des Marais, D., 2000. The role of microbes in accretion, lamination and early lithification of modern marine stromatolites. *Nature (Lond.)* 406, 989–992.
- Rippka, R., Deruelles, J., Waterbury, J.B., Herdman, J., Stanier, R.Y., 1979. Generic assignments, strain histories and properties of pure cultures of Cyanobacteria. *J. Gen. Microbiol.* 111, 1–61.
- SAS Institute, 1985. *SAS user's guide: statistics*, version 5 edition. SAS Institute, Cary, NC.
- Sawyer, T.E., King, G.M., 1993. Glucose uptake in an intertidal marine sediment: metabolism and endproduct formation. *Appl. Environ. Microbiol.* 59, 120–128.
- Schopf, J.W., 1996. Are the oldest fossils Cyanobacteria. In: Roberts, D.M., Sharp, P., Alderson, G., Collins, M. (Eds.), *Evolution of Microbial Life*. Cambridge Univ. Press, Washington, DC, pp. 23–62.
- Smith, D.J., Underwood, G.J.C., 1998. Exopolymer production by intertidal epipellic diatoms. *Limnol. Oceanogr.* 43, 1578–1591.
- Smith, D.J., Underwood, G.J.C., 2000. The production of extracellular carbohydrates by estuarine benthic diatoms: the effects of growth phase and light and dark treatment. *J. Phycol.* 36, 321–333.
- Staats, N., Stal, L.J., de Winder, B., Mur, L.R., 2000. Oxygenic photosynthesis as a driving process in exopolysaccharide production in benthic diatoms. *Mar. Ecol., Prog. Ser.* 193, 261–269.
- Stal, L.J., 1991. The metabolic diversity of the mat-building cyanobacterium *Microcoleus chthonoplastes* and *Oscillatoria limosa* and its ecological significance. *Algol. Stud.* 64, 453–467.
- Stal, L.J., 1995. Physiological ecology of Cyanobacteria in microbial mats and other communities. *New Phytol.* 131, 1–32.
- Stal, L.J., 2000. Cyanobacterial mats and stromatolites. In: Whitton, B.A., Potts, M. (Eds.), *The Ecology of Cyanobacteria*. Kluwer Acad. Press, Dordrecht, pp. 61–120.
- Stolz, J.F., 2000. Structure of microbial mats and biofilms. In: Riding, R.E., Awramik, S.M. (Eds.), *Microbial Sediments*. Springer-Verlag, Berlin, pp. 1–8.
- Taylor, I.S., Paterson, D.M., 1998. Micropatial variation in carbohydrate concentrations with depth in the upper millimetres of intertidal cohesive sediments. *Estuar. Coast. Shelf Sci.* 46, 359–370.
- Taylor, I.S., Paterson, D.M., Mehlert, A., 1999. The quantitative variability and monosaccharide composition of sediment carbohydrates associated with intertidal diatom assemblages. *Biogeochemistry* 45, 303–327.
- Underwood, G.J.C., Kromkamp, J., 1999. Primary production by phytoplankton and microphytobenthos in estuaries. *Adv. Ecol. Res.* 29, 93–153.
- Underwood, G.J.C., Paterson, D.M., Parkes, R.J., 1995. The measurement of microbial carbohydrate exopolymers from intertidal sediments. *Limnol. Oceanogr.* 40, 1243–1253.
- Underwood, G.J.C., Nilsson, C., Sundbäck, K., Wulff, A., 1999. Short-term effects of UVB irradiation on chlorophyll fluorescence, biomass, pigments and carbohydrate fractions in a benthic diatom mat. *J. Phycol.* 35, 656–666.
- Van den Ende, F.P., Van Gernerden, H., 1993. Sulfide oxidation under oxygen-limitation by a *Thiobacillus thioparus* isolated from a marine microbial mat. *FEMS Microbiol. Ecol.* 13, 69–78.
- Visscher, P.T., Prins, R.A., Van Gernerden, H., 1992. Rates of sulfate reduction and thiosulfate consumption in a marine microbial mat. *FEMS Microbiol. Ecol.* 86, 283–394.
- Visscher, P.T., Reid, R.P., Bebout, B.M., Hoeff, S.E., MacIntyre, I.G., Thompson, J.A., 1998. Formation of lithified micritic laminae in modern marine stromatolites (Bahamas): the role of sulfur cycling. *Am. Mineral.* 83, 1482–1493.
- Visscher, P.T., Gritzer, F.R., Leadbetter, E.R., 1999. Low-molecular weight sulfonates, a major substrate for sulfate reducers in marine microbial mats. *Appl. Environ. Microbiol.* 65, 3272–3278.
- Visscher, P.T., Reid, R.P., Bebout, B.M., 2000. Microscale observations of sulfate reduction: correlation of microbial activity with lithified micritic laminae in modern marine stromatolites. *Geology* 28, 919–922.
- Visscher, P.T., Surgeon, T.M., Hoeff, S.E., Bebout, B.M., Thompson Jr., J., Reid, R.P., 2002. Microelectrode studies in modern marine stromatolites: unraveling the Earth's past? In: Taillefert, M., Rozan, T. (Eds.), *Environmental Electrochemistry: Analyses of Trace Element Biogeochemistry*, Am. Chem. Soc. Symp. Ser., vol. 811. Oxford Univ Press, New York, NY, pp. 265–282.
- Weaver, D.T., Hicks, R.E., 1995. Biodegradation of *Azotobacter vinelandii* exopolymer by Lake Superior microbes. *Limnol. Oceanogr.* 40, 1035–1041.
- Wolfstein, K., Stal, L.J., 2002. The production of extracellular polymeric substances (EPS) by benthic diatoms: the effect of irradiance and temperature. *Mar. Ecol., Prog. Ser.* 245, 13–21.
- Wolfstein, K., De Bouwer, J.F.C., Stal, L.J., 2002. Biochemical partitioning of photosynthetically fixed carbon by benthic diatoms during short-term incubations at different irradiances. *Mar. Ecol., Prog. Ser.* 245, 22–31.
- Wolter, K., 1982. Bacterial incorporation of organic substances released by natural phytoplankton populations. *Mar. Ecol., Prog. Ser.* 7, 287–295.